

Magnetic Reconnection and Energy Extraction from a Konoplya-Zhidenko rotating non-Kerr black hole

Fen Long^{1*}, Shangyun Wang^{2†}, Songbai Chen^{3,4‡}, Jiliang Jing^{3,4 §}

¹ *School of Mathematics and Physics, University of South China, Hengyang, 421001, China*

² *College of Physics and Electronic Engineering,
Hengyang Normal University, Hengyang 421002, China*

³ *Department of Physics, Institute of Interdisciplinary Studies,
Key Laboratory of Low Dimensional Quantum Structures and Quantum Control of Ministry of Education,
Synergetic Innovation Center for Quantum Effects and Applications,
Hunan Normal University, Changsha, Hunan 410081, People's Republic of China*

⁴ *Center for Gravitation and Cosmology, College of Physical Science and Technology,
Yangzhou University, Yangzhou 225009, People's Republic of China*

Abstract

Recently, magnetic reconnection has attracted considerable attention as a novel energy extraction mechanism, relying on the rapid reconnection of magnetic field lines within the ergosphere. We have investigated the properties of the energy extraction via magnetic reconnection in a Konoplya-Zhidenko rotating non-Kerr black hole spacetime with an extra deformation parameter. Our results show that the positive deformation parameter expands the possible region of energy extraction and improves the maximum power, maximum efficiency, and the maximum ratio of energy extraction between magnetic reconnection and the Blandford-Znajek process. This means that in the Konoplya-Zhidenko rotating non-Kerr black hole spacetime one can extract more energy via magnetic reconnection than in the Kerr black hole case. These effects of the deformation parameter may provide valuable clues for future astronomical observations of black holes and verification of gravity theories.

PACS numbers:

* lf@usc.edu.cn

† sywang@hynu.edu.cn

‡ csb3752@hunnu.edu.cn

§ jljing@hunnu.edu.cn

I. INTRODUCTION

General relativity theoretically predicts the existence of black holes, and observations of gravitational waves [1–5] as well as black hole images [6, 7] provide favorable experimental evidence for confirming their existence, which ushering in a golden age of black hole physics research. Black holes, as the most fascinating and intriguing entities in astrophysics, are notable not only for their extremely curved geometry and intensely strong gravitational field but also for their pivotal role in explaining high-energy astrophysical phenomena, such as active galactic nuclei (AGN)[8–11], gamma-ray bursts (GRB) [12–14], and ultraluminous X-ray binaries [15], where an enormous amount of energy is released. Exploring the mechanisms of energy extraction from black holes helps to uncover the underlying principles behind the generation of high-energy astrophysical phenomena.

The most famous mechanism for extracting energy from black holes is the Penrose process [16], where the energy is extracted from a rotating black hole through particle splitting. The incident particle 1 entering the ergosphere splits into two particles 2 and 3. Subsequently, the particle 2 with negative energy passes across the outer horizon and falls into the black hole, while the particle 3 escapes to infinity with more energy than that of the incident particle 1. However, this process requires that the relative three-velocity between the particles 2 and 3 must satisfy the condition $v > c/2$ [17], which is relatively difficult to achieve experimentally. At the same time, in order to achieve the highest possible energy extraction efficiency, particles split as close to the event horizon as possible. Since these conditions are difficult to achieve and sustain in nature, the Penrose process is insufficient to explain high-energy astrophysical phenomena. The magnetic Penrose process (MPP) [18] indicates that when a black hole is surrounded by a magnetic field, the relative velocity condition for particle splitting is easily satisfied, and the energy extraction efficiency of the MPP exceeds 100% in realistic settings [19, 20]. The Blandford-Znajek (BZ) [21] process utilizes the interaction between a black hole and its surrounding electromagnetic field to extract rotational energy from the rotating black hole, rather than through particle splitting. Therefore, the MPP and BZ process are considered as excellent models for explaining the energy mechanism of active galactic nucleus jets and gamma-ray burst central engines. In addition to the three mechanisms mentioned above, there are several well-known energy extraction mechanisms, such as collisional Penrose process [22], the magnetohydrodynamic Penrose process [23], Superradiant scattering [24] and so on.

Besides the previously mentioned mechanisms, recent researches (Koide and Arai [25]; Comisso and Asenjo [26]) proposed a new mechanism for energy extraction from the ergosphere of the rotating black holes via mag-

netic reconnection. Magnetic reconnection occurs in the plasma rotating around a black hole in the equatorial plane. The frame-dragging effect generated by rapidly spinning black hole creates adjacent antiparallel magnetic field on the equatorial plane. This creates an equatorial current sheet is prone to fast plasmoid-mediated magnetic reconnection, which converts magnetic energy into kinetic energy of the plasma and generates a pair of plasma outflows in opposite directions in the reconnection layer [26]. One part of the plasma carries a lot of negative energy and falls into the black hole event horizon along retrograde orbit, while the other part of the plasma with positive energy escapes to infinity along prograde orbit, thus achieving energy extraction. Comisso and Asenjo [26] show that under conditions of high spin and strong magnetization of the plasma in Kerr black hole, the maximum efficiency of the energy extraction via magnetic reconnection in the ergosphere can reach $3/2$ [26]. Researchs on energy extraction via magnetic reconnection have extended to various rotating compact objects [27–40], which provides valuable material for verifying gravity theories.

In this paper, we will study energy extraction via magnetic reconnection in Konoplya-Zhidenko rotating non-Kerr black hole [41]. The Konoplya-Zhidenko rotating non-Kerr metric exhibits some non-negligible deviation from Kerr spacetime. It has been found that the Kerr metric with these deviations can also yield the same frequencies of black-hole ringing [41], which leaves a window open for the alternative theories beyond general relativity. Moreover, the constraints from quasi-periodic oscillations [42] and the iron line [43] also support that a real astrophysical black hole could be described by Konoplya-Zhidenko rotating non-Kerr metric. Therefore, it is necessary to further explore the features of the Konoplya-Zhidenko rotating non-Kerr metric through various processes to distinguish this theory from general relativity. The energy extraction via the Penrose process in Konoplya-Zhidenko rotating non-Kerr black holes [44] show that the maximum efficiency of the energy extraction process of black hole with superspinning is greatly improved when the deformation parameter is close to zero, which is much higher than the Kerr case. Therefore, we will investigate energy extraction via magnetic reconnection in the Konoplya-Zhidenko rotating non-Kerr black hole, analyzing the impact of the deformation parameter on energy extraction efficiency. We will then compare the results with those from energy extraction via magnetic reconnection in the Kerr black hole and the Penrose process in a Konoplya-Zhidenko rotating non-Kerr black hole. This comparison will allow us to examine the differences in energy extraction between these different black holes and processes, and to provide insights into their distinct characteristics, which offers additional information and multiple perspectives to test the deviation from Kerr black hole in general relativity.

This paper is organized as follows. In Sec.II, we briefly review the metric of the Konoplya-Zhidenko rotating

non-Kerr black hole and calculated several characteristic orbital radii related to energy extraction, including the horizon radius, the redshift radius, and the photosphere radius. In Sec.III, we investigate the magnetic reconnection of Konoplya-Zhidenko rotating non Kerr black hole and clarify the possible parameter regions where energy extraction can occur. In Sec.IV, we calculate the power and efficiency via magnetic reconnection. Finally, we present a brief summary.

II. THE KONOPLYA-ZHIDENKO ROTATING NON-KERR BLACK HOLE SPACETIME

In the Boyer-Lindquist coordinates, the metric of a Konoplya-Zhidenko rotating non-Kerr black hole can be written as follows [41]:

$$ds^2 = - \left(1 - \frac{2Mr + \frac{\eta}{r}}{\rho^2} \right) dt^2 + \frac{\rho^2}{\Delta} dr^2 + \rho^2 d\theta^2 + \frac{A}{\rho^2} \sin^2 \theta d\phi^2 - \frac{2(2Mr + \frac{\eta}{r}) a \sin^2 \theta}{\rho^2} dt d\phi, \quad (1)$$

with

$$\rho^2 = r^2 + a^2 \cos^2 \theta, \quad \Delta = r^2 - 2Mr + a^2 - \frac{\eta}{r}, \quad A = (r^2 + a^2)^2 - a^2 \Delta \sin^2 \theta, \quad (2)$$

where M denotes the mass of black hole and a represents the rotation parameter. The deformation parameter η describes the deviations from the Kerr spacetime. When the deformation parameter absent, this metric reduces to the Kerr black hole. Obviously, the presence of the deformation parameter η does not change the asymptotic structure of spacetime at the spatial infinite, but modifies the behavior of spacetime in the strong field region.

Initially, we will perform a detailed analysis of a series of characteristic surfaces and their orbital radii related to magnetic reconnection and energy extraction, including the horizon, the the infinite redshift surface, and the photosphere. The region of the ergosphere defined by the outer event horizon and the outer infinite redshift surface is where magnetic reconnection occurs, making it crucial for extracting rotational energy from a rotating black hole. For a Konoplya-Zhidenko rotating non-Kerr black hole, the horizons of the black hole are defined by the equation

$$r^3 - 2Mr^2 + a^2 r - \eta = 0, \quad (3)$$

and the infinite redshift surface is defined by the equation

$$r^3 - 2Mr^2 + a^2 r \cos^2 \theta - \eta = 0. \quad (4)$$

The variation of the event horizon radius and the infinite redshift surface with the deformation parameter η in the Konoplya-Zhidenko rotating non-Kerr black hole was discussed [44]. As η increases, the ergosphere in

the equatorial plane becomes thinner. In the case of $a > M$ and when positive η approaches zero, the outer horizon radius becomes very small, making the ergosphere in the equatorial plane much thicker than in the case of $a < M$. At this point, the maximum efficiency of Penrose process in this rotating non-Kerr black hole become almost unlimited.

Another characteristic orbit plays an important role in magnetic reconnection, which is the photon orbit with $\mu = 0$. The Hamiltonian of a photon propagation along null geodesics in a Konoplya-Zhidenko rotating non-Kerr black hole spacetime can be expressed as

$$H(x, p) = \frac{1}{2} g^{\mu\nu}(x) p_\mu p_\nu = 0. \quad (5)$$

There are two conserved quantities for photon propagation: E , the energy of the photon, and L_ϕ , its angular momentum in the ϕ direction.

$$\begin{aligned} E &= -p_t = -g_{tt}\dot{t} - g_{t\phi}\dot{\phi}, \\ L_\phi &= p_\phi = g_{t\phi}\dot{t} + g_{\phi\phi}\dot{\phi}. \end{aligned} \quad (6)$$

With these conserved quantities, the null geodesics for a photon can be further simplified as

$$\frac{dt}{d\tau} = E + \frac{(a^2 E - aL_\phi + Er^2)(2Mr^2 + \eta)}{\Delta\rho^2 r} \quad (7)$$

$$\frac{d\phi}{d\tau} = \frac{aE \sin^2 \theta (2Mr^2 + \eta) + a^2 L_\phi r \cos^2 \theta - L_\phi (2Mr^2 - r^3 + \eta)}{\Delta\rho^2 r \sin^2 \theta}, \quad (8)$$

$$\rho^4 \left(\frac{dr}{d\tau} \right)^2 = R(r) = -\Delta K + [aL_\phi - (r^2 + a^2) E]^2, \quad (9)$$

$$\rho^4 \left(\frac{d\theta}{d\tau} \right)^2 = \Theta = K - \frac{1}{\sin^2 \theta} (L_\phi - aE \sin^2 \theta)^2, \quad (10)$$

where the quantity K is the constant of separation associating with the hidden symmetries of the spacetime. According to the conditions for photon circular orbits $R(r) = 0$ and $R'(r) = 0$, combined with the definition of impact parameters $\xi = \frac{L_\phi}{E}$ and $\sigma = \frac{K}{E^2}$, one can obtain

$$\begin{aligned} \xi &= \frac{a^2 (\eta - 2Mr^2 - 2r^3) + 6Mr^4 + 5\eta r^2 - 2r^5}{a(2r^3 - 2Mr^2 + \eta)}, \\ \sigma &= \frac{16r^5 (r^3 + a^2 r - 2Mr^2 - \eta)}{(2r^3 - 2Mr^2 + \eta)^2}. \end{aligned} \quad (11)$$

For the case of photon propagates on the equatorial plane, its motion satisfies

$$\Theta|_{\theta=\frac{1}{2}} = 0. \quad (12)$$

From Eqs. (10), (11) and (12), we find that the radius r_{ph} of the unstable photon circular orbits on the

equatorial plane can be given by

$$(2r^3 - 6Mr^2 - 5\eta)^2 - 8a^2(2Mr^3 + 3\eta r) = 0. \quad (13)$$

This study is based on the simplified assumption that magnetic reconnection occurs in plasma rotating along circular orbits around a black hole in the equatorial plane. According to the above conditions for circular orbits and the r -component of the Euler-Lagrange equation, the Keplerian angular velocity $\Omega_K = \frac{d\phi/d\tau}{dt/d\tau}$ can be expressed as

$$\Omega_K = \frac{\sqrt{2Mr^2 + 3\eta}}{a\sqrt{2Mr^2 + 3\eta} \pm \sqrt{2r^5}}. \quad (14)$$

The upper sign indicates prograde orbits, whereas the lower sign corresponds to retrograde orbits.

III. ENERGY EXTRACTION VIA MAGNETIC RECONNECTION MECHANISM

In this section, we will investigate the energy extraction of the Konoplya-Zhidenko rotating non-Kerr black hole under magnetic reconnection, and analyze the influence of the deformation parameter on energy extraction and further explore the differences by comparing the research results with those in the Kerr case. For convenience, we will calculate and analyze the plasma energy density in the Zero Angular Momentum Observer (ZAMO) frame. The line element in this frame appears as in Minkowski spacetime, written as

$$ds^2 = -d\hat{t}^2 + \sum_{i=1}^3 (d\hat{x}^i)^2 = \eta_{\mu\nu} d\hat{x}^\mu d\hat{x}^\nu, \quad (15)$$

The transformation between the BL frame (dt, dx^1, dx^2, dx^3) and the ZAMO frame $(d\hat{t}, d\hat{x}^1, d\hat{x}^2, d\hat{x}^3)$ is expressed as

$$d\hat{t} = \alpha dt, \quad d\hat{x}^i = \sqrt{g_{ii}} dx^i - \alpha \beta^i dt, \quad (16)$$

where

$$\alpha = \sqrt{-g_{tt} + \frac{g_{\phi t}^2}{g_{\phi\phi}}} = \left(\frac{\Delta \rho^2}{A} \right)^{1/2}, \quad \beta^\phi = \frac{\sqrt{g_{\phi\phi}} \omega^\phi}{\alpha} = \frac{\omega^\phi}{\alpha} \left(\frac{A}{\rho^2} \right)^{1/2} \sin \theta, \quad (17)$$

here α is the lapse function, $\beta^i = (0, 0, \beta^\phi)$ is the shift vector, and $\omega^\phi = -g_{\phi t}/g_{\phi\phi}$ means the angular velocity of the frame dragging. According to Equation (16), we can obtain the transformation of vectors between the two frames as follows:

$$\hat{\psi}^0 = \alpha \psi^0, \quad \hat{\psi}^i = \sqrt{g_{ii}} \psi^i - \alpha \beta^i \psi^0. \quad (18)$$

During magnetic reconnection, the breaking and reconnection of magnetic field lines release a substantial amount of energy, and the plasma escapes from the reconnection layer with this energy. When part of the plasma carrying negative energy fall into the black hole, while another part carrying positive energy manages to escape the black hole and travel to infinity, it is possible to steal energy from the black hole. Next, we would like to analyze the feasibility conditions for energy extraction from the Konoplya-Zhidenko rotating non-Kerr black hole via magnetic reconnection. Under the one-fluid approximation, the energy-momentum tensor $T^{\mu\nu}$ of the plasma, can be expressed as

$$T^{\mu\nu} = pg^{\mu\nu} + wU^\mu U^\nu + F_\delta^\mu F^{\nu\delta} - \frac{1}{4}g^{\mu\nu}F^{\rho\delta}F_{\rho\delta}, \quad (19)$$

here, p , w , U^μ and $F^{\mu\nu}$ respectively represent plasma pressure, enthalpy density, 4-velocity and electromagnetic tensor. According to definition of the ‘‘energy-at-infinity’’ density, we have

$$e^\infty = -\alpha g_{\mu 0} T^{\mu 0} = \alpha \hat{e} + \alpha \beta^\phi \hat{P}^\phi, \quad (20)$$

where the total energy density \hat{e} and the azimuthal component of the momentum density \hat{P}^ϕ are given by

$$\begin{aligned} \hat{e} &= w\hat{\gamma}^2 - p + \frac{\hat{B}^2 + \hat{E}^2}{2}, \\ \hat{P}^\phi &= w\hat{\gamma}^2 \hat{v}^\phi + (\hat{B} \times \hat{E})^\phi, \end{aligned} \quad (21)$$

here, $\hat{\gamma} = \hat{U}^0 = \left[1 - \sum_{i=1}^3 (d\hat{v}^i)^2\right]^{-1/2}$, $\hat{B}^i = \epsilon^{ijk} \hat{F}_{jk}/2$, $\hat{E}^i = \eta^{ij} \hat{F}_{j0} = \hat{F}_{i0}$ and \hat{v}^ϕ respectively represent the Lorentz factor, the components of the electric and magnetic fields, and the velocity of the plasma flowing out of the reconnection layer in the ZAMO frame.

The energy-at-infinity density could be separated into $e^\infty = e_{hyd}^\infty + e_{em}^\infty$, where e_{hyd}^∞ and e_{em}^∞ represent the hydrodynamic component and the electromagnetic component, respectively, and they are given by

$$e_{hyd}^\infty = \alpha \hat{e}_{hyd} + \alpha \beta^\phi \omega \hat{\gamma}^2 \hat{v}^\phi, \quad (22)$$

$$e_{em}^\infty = \alpha \hat{e}_{em} + \alpha \beta^\phi (\hat{B} \times \hat{E})_\phi. \quad (23)$$

\hat{e}_{hyd} and \hat{e}_{em} are respectively the hydrodynamic and electromagnetic energy densities in the ZAMO frame. Considering that in the magnetic reconnection process, most of the magnetic energy is converted into the kinetic energy of the plasma, the contribution of e_{em}^∞ in the total energy can be ignored, which leads to $e^\infty \approx e_{hyd}^\infty$. Additionally, assuming that the plasma element is incompressible and adiabatic, the energy-at-infinity density can be rewritten as[25]

$$e^\infty = \alpha \omega \hat{\gamma} \left(1 + \beta^\phi \hat{v}^\phi\right) - \frac{\alpha p}{\hat{\gamma}}. \quad (24)$$

For the convenience of analyzing local reconnection process, one can introduce the local rest frame $x^{\mu'} = (x^{0'}, x^{1'}, x^{2'}, x^{3'})$ to study the bulk plasma rotating with Keplerian angular velocity in the equatorial plane, where the directions of $x^{1'}$ and $x^{3'}$ in the local rest frame are parallel to the radial $x^1 = r$ and azimuthal direction $x^3 = \phi$, respectively. According to the transformation Equation (16), the Keplerian angular velocity observed in the ZAMO frame is given by

$$\hat{v}_K = \frac{d\hat{x}^\phi}{d\hat{x}^t} = \frac{\sqrt{g_{\phi\phi}}dx^\phi - \alpha\beta^\phi dx^t}{\alpha dx^t} = \frac{\sqrt{g_{\phi\phi}}}{\alpha}\Omega_K - \beta^\phi. \quad (25)$$

Considering "relativistic adiabatic incompressible ball approach" and assuming a relativistically hot plasma with a polytropic index $\Gamma = 3/4$, the energy at infinity per enthalpy can be expressed in accordance with $\epsilon_{\pm}^\infty = e^\infty/w$ as follows[26]:

$$\epsilon_{\pm}^\infty = \alpha\hat{\gamma}_K \left[(1 + \beta^\phi\hat{v}_K) \sqrt{1 + \sigma_0} \pm \cos\xi (\beta^\phi + \hat{v}_K) \sqrt{\sigma_0} - \frac{\sqrt{1 + \sigma_0} \mp \cos\xi\hat{v}_K\sqrt{\sigma_0}}{4\hat{\gamma}_K^2(1 + \sigma_0 - \cos^2\xi\hat{v}_K^2\sigma_0)} \right], \quad (26)$$

where symbols + and - represent plasma particles undergoing acceleration and deceleration, respectively escaping from the reconnection layer with co-rotating and counter-rotating outflow directions. The corresponding Lorentz factor denoted as $\hat{\gamma}_K = 1/\sqrt{1 - \hat{v}_K^2}$. The plasma magnetization upstream of the reconnection layer is given by $\sigma_0 = B_0^2/w_0$. From Eq.(26), we can deduce that the hydrodynamic energy at infinity per enthalpy is a function of the critical parameters $(a, M, \eta, \sigma_0, \xi, r)$, where r indicates the location of the reconnection point, denoted as the X-point. Additionally, ξ represents the orientation angle between the magnetic field lines and the azimuthal direction in the equatorial plane. Many studies have shown that the energy-at-infinity per enthalpy via magnetic reconnection favors smaller values of the angle ξ [27, 32, 33]. Therefore, we sets $\xi = \pi/12$ to study the effect of deformation parameters η on energy extraction. The existence of deformation parameters in the Konoplya-Zhidenko rotating non-Kerr black hole expands the range of the rotation parameter a , allowing it to be greater than M . When the rotation parameter $a > M$, the deformation parameter must satisfy the condition $\eta > 0$; When the rotation parameter $a < M$, the deformation parameter must satisfy the condition $\eta > \eta_c = -\frac{2}{27}(\sqrt{4M^2 - 3a^2} + 2M)^2(\sqrt{4M^2 - 3a^2} - M)$ to ensure the existence of the horizon and the ergosphere, which is crucial for energy extraction.

In Fig.1, we present the change of the energy at infinity per enthalpy ϵ_{\pm}^∞ with the plasma magnetization parameter σ_0 for different rotation parameter a , dominant X-point location r and deformation parameter η . We take the value of a and η in the range where the existence of the horizon is ensured. Fig.1 shows that regardless of the values of the rotation parameter and the deformation parameter, the energy at infinity per enthalpy ϵ_+^∞ increases with the plasma magnetization parameter σ_0 , while ϵ_-^∞ decreases except the region

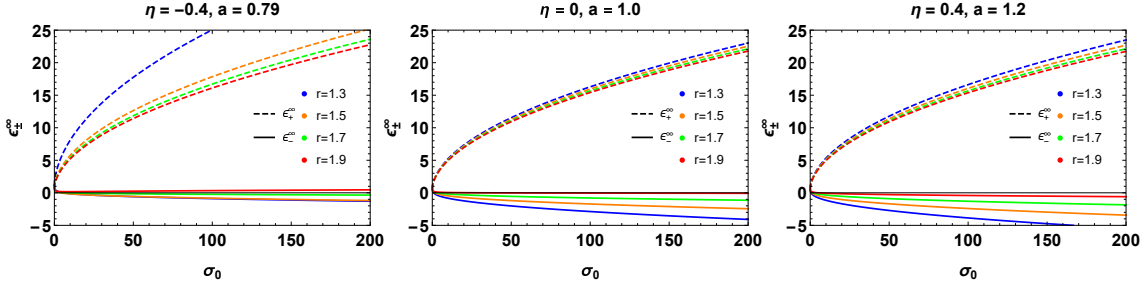


FIG. 1: The change of the energy at infinity per enthalpy ϵ_{\pm}^{∞} with the plasma magnetization parameter σ_0 for different rotation parameter a , dominant X-point location r and deformation parameter η , we set $M = 1$.

where σ_0 is small. Therefore, we assume that the ion magnetization parameter $\sigma_0 = 100$ to investigate the influence of deformation parameters η on the energy at infinity per enthalpy ϵ_{\pm}^{∞} .

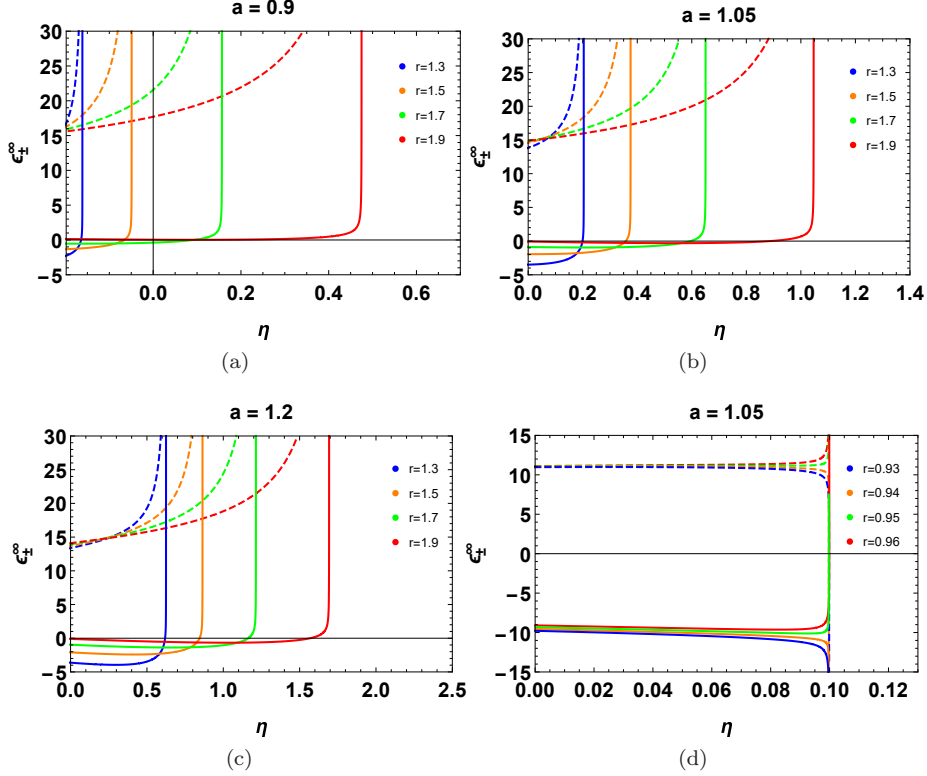


FIG. 2: The change of the energy at infinity per enthalpy ϵ_{\pm}^{∞} with the deformation parameter η for different rotation parameter a and dominant X-point location r . The dashed and solid lines correspond to the energy at infinity per enthalpy ϵ_{+}^{∞} and ϵ_{-}^{∞} . We set $\sigma_0 = 100$ and $M = 1$.

In Fig.2, we present the change of the energy at infinity per enthalpy ϵ_{\pm}^{∞} with the deformation parameter η for different rotation parameter a . We found that when the value of the dominant X-point location r is slightly greater than M , the energy at infinity per enthalpy of the accelerated plasma ϵ_{+}^{∞} increases with the deformation parameters η ; the decelerated part ϵ_{-}^{∞} slowly increases with the deformation parameter in the cases $a = 0.9$

and $a = 1.05$, but it first slowly decreases and then sharply increases with the deformation parameter in the case with $a = 1.2$. It is worth noting that when the rotation parameter $M < a \leq \frac{2\sqrt{3}}{3}M \approx 1.155M$ and the dominant X-point location is slightly greater(or smaller) than r_c which is determined by the maximum(or second largest) value in the numerical solution of equation $a\sqrt{2Mr_c^3 + 3\eta_cr_c} + \sqrt{2}(r_c^3 - 2Mr_c^2 - \eta_c) = 0$, the values of the energy at infinity per enthalpy of the accelerated plasma ϵ_+^∞ and the decelerated part ϵ_-^∞ are close to opposite numbers, so their sum tends to be close to zero. This implies that ϵ_+^∞ is much greater than the sum of ϵ_+^∞ and ϵ_-^∞ , which is different from the characteristics in Kerr black holes and may introduce new features to the energy extraction results of the Konoplya-Zhidenko rotating non-Kerr black hole. Similarly to the Penrose process, in order to extract energy from the black hole through magnetic reconnection, it is anticipated that the decelerated plasma should exhibit negative energy as observed at infinity, while the accelerated plasma is expected to have positive energy, surpassing its rest mass and thermal energy. Thus, the conditions of extracting energy can be expressed as [26]

$$\epsilon_-^\infty < 0, \quad \text{and} \quad \Delta\epsilon_+^\infty = \epsilon_+^\infty - \left(1 - \frac{\Gamma}{\Gamma - 1} \frac{p}{\omega}\right) = \epsilon_+^\infty > 0. \quad (27)$$

From Fig.2, it can be seen that the value of the energy at infinity per enthalpy of the accelerated plasma ϵ_+^∞ in the Konoplya-Zhidenko rotating non-Kerr black hole is always positive, so we only need to consider the condition $\epsilon_-^\infty < 0$.

To study energy extraction via the magnetic reconnection mechanism, it is essential to clarify the possible parameter regions where energy extraction can occur. We have combined the outer horizon, photosphere, outer infinite redshift surface, and the energy conditions from Eq.(27) to create Fig.3 and Fig.4, further analyzing the effects of the plasma magnetization parameter σ_0 , the rotating parameter a and deformation parameter η on these possible parameter regions of the phase space (a, r) and (η, r) . The blue shaded areas from light to dark in the figures represent the regions corresponding to the plasma magnetization parameter $\sigma_0 = 1, 5, 10, 100$ that satisfy the condition $\epsilon_-^\infty < 0$. Fig.3 and Fig.4 shows the possible regions expand with increasing parameter σ_0 which is the same as in the Kerr case. A portion of the blue shaded areas lies below the outer horizon, indicating that their radii are smaller than the outer horizon's. Therefore, this part cannot achieve energy extraction and should be excluded from the possible regions. We primarily focus on the blue shaded areas with radii situated in the ergosphere, between the outer horizon and the infinite redshift surface. In Fig.3, for the case with $\eta \leq 0$, under the condition of the ergosphere, most of the blue shaded areas on the right and below that are located without the outer horizon must be excluded. As the deformation parameter

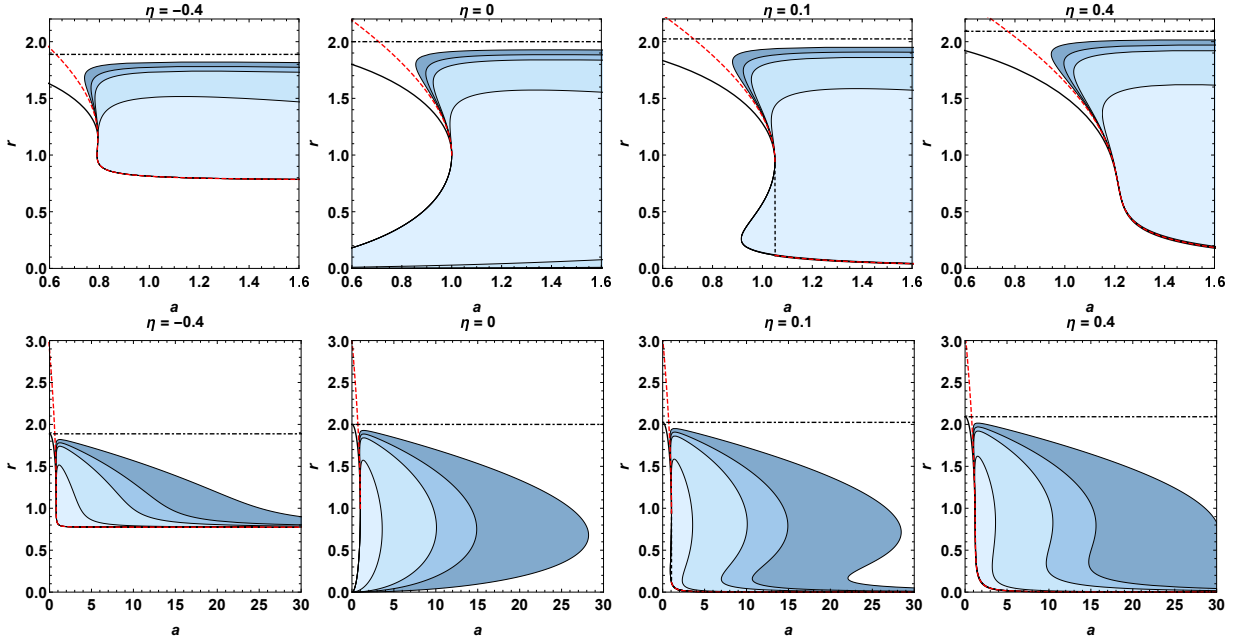


FIG. 3: Regions of the phase space (a, r) that satisfy the condition $\epsilon^\infty < 0$. The blue shaded areas from light to dark correspond to $\epsilon_+^\infty > 0$ for the plasma magnetization parameter $\sigma_0 = 1, 5, 10, 100$. The thick black solid line, red dashed line, and dot-dashed line correspond to the radius of the outer horizon, photosphere, and the outer infinite redshift surface, respectively. We set $M = 1$.

η decreases, the possible regions of the phase space (a, r) gradually shift to the upper left and contract, becoming smaller than the possible region in the Kerr case. In this scenario, the dominant X-point location needs to satisfy $r \geq M$ and $a \leq M$. For the case with $\eta > 0$, the ergosphere exists for $a > M$ and the possible region expands to $r < M$ and $a > M$, which extends beyond the phase space (a, r) in the Kerr black hole. Especially when $0 < \eta < \frac{8}{27}$, as the rotating parameter a increase, the outer horizon and photosphere radii will experience a sharp drop to very small values, and the possible region of the phase space (a, r) will rapidly expand to the range with small r . This situation of thick ergosphere and small X-points will yield unique results for energy extraction research in the Konoplya-Zhidenko rotating non-Kerr black hole. In Fig.4, as the rotating parameter a increases, the possible regions of the phase space (η, r) gradually shift to the upper right and expand. For a highly rotating black hole with $a > M$ and the positive deformation parameter approaches to zero, the possible region (η, r) can expand to a radius r that is very small or even close to zero. Especially when $M < a < \frac{2\sqrt{3}}{3}M$, the radius of outer horizon and photosphere increases abruptly with the deformation parameter, and the possible region (η, r) forms a narrow strip near $\eta = 0$. To conclude, the existence of the deformation parameter η in the Konoplya-Zhidenko rotating non-Kerr black hole significantly expands the possible regions for energy extraction via the magnetic reconnection mechanism, extending into the areas where $a > M$ and $r < M$ that have not been involved in the Kerr black hole case. The energy

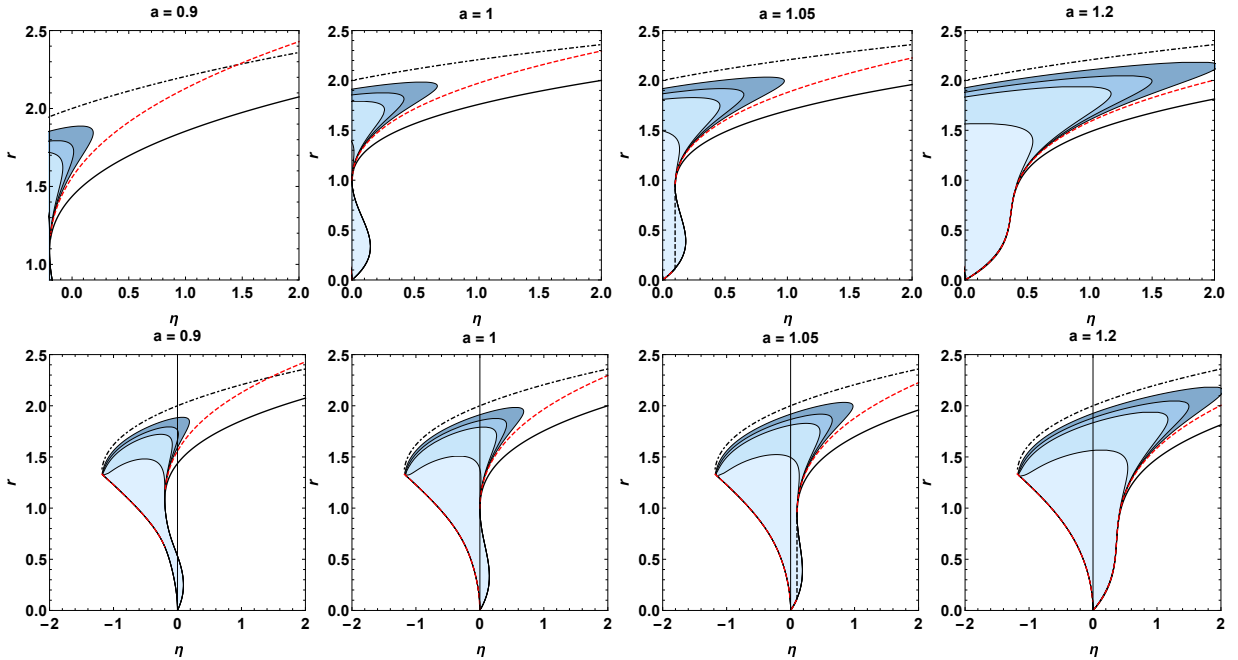


FIG. 4: Regions of the phase space (η, r) that satisfy the condition $\epsilon_{\infty}^{\infty} < 0$. The blue shaded areas from light to dark correspond to $\epsilon_{+}^{\infty} > 0$ for the plasma magnetization parameter $\sigma_0 = 1, 5, 10, 100$. The thick black solid line, red dashed line, and dot-dashed line correspond to the radius of the outer horizon, photosphere, and the outer infinite redshift surface, respectively. We set $M = 1$.

extraction power and efficiency through magnetic reconnection in this region are likely to exhibit fascinating characteristics.

IV. POWER AND EFFICIENCY VIA MAGNETIC RECONNECTION

In this section, we will investigate energy extraction from a Konoplya-Zhidenko rotating non-Kerr black hole via magnetic reconnection and analyze the impact of the deformation parameter η on both the energy extraction power and efficiency. It is important to emphasize that both energy efficiency and power depend on the negative energy of decelerated plasma absorbed by a black hole within a unit of time. The power P_{extr} of energy extraction per enthalpy via magnetic reconnection from Konoplya-Zhidenko rotating non-Kerr black hole can be evaluated as [26]

$$P_{\text{extr}} = -\epsilon_{-}^{\infty} w_0 A_{\text{in}} U_{\text{in}}, \quad (28)$$

where the reconnection in flow four-velocity $U_{\text{in}} = \mathcal{O}(10^{-1})$ and $\mathcal{O}(10^{-2})$ for the collisionless and collisional regimes. The cross-sectional area of the inflowing plasma A_{in} can be estimated as $A_{\text{in}} \sim (r_{\infty}^2 - r_{\text{ph}}^2)$. From Eq.(28), it can be seen that power is related to four parameters: the deformation parameter η , the rotation parameter a , the dominant X-point location r and the plasma magnetization parameter σ_0 . In Fig.5,

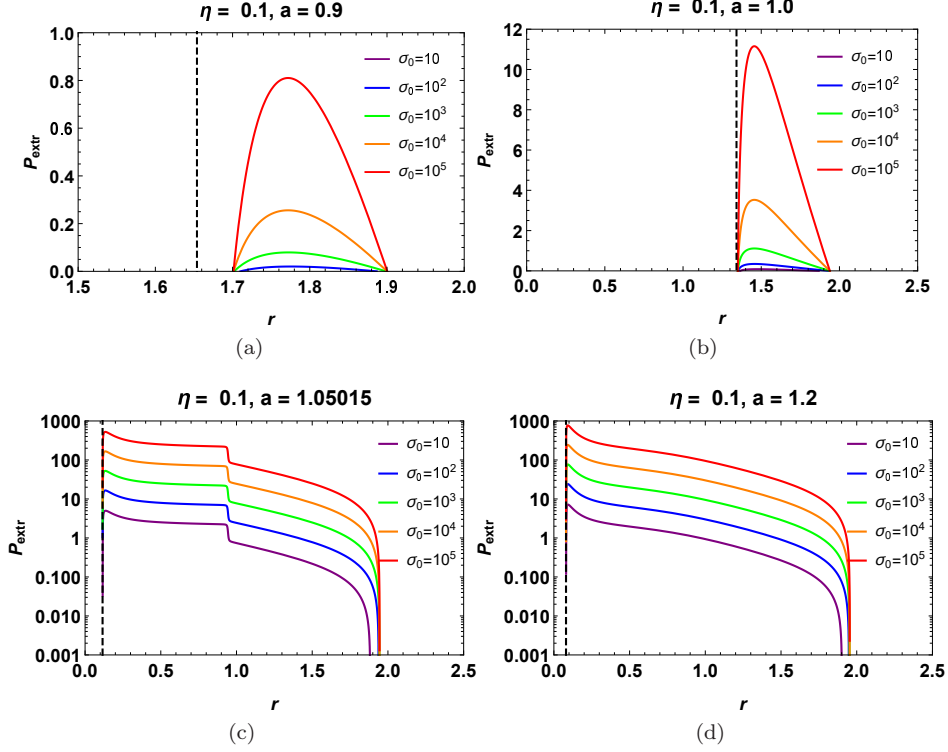


FIG. 5: The change of power P_{extr} with the dominant X-point location r for different rotation parameter a and plasma magnetization parameter σ_0 . The black dashed lines represent the photosphere r_{ph} . We set $M = 1$.

with the deformation parameter $\eta = 0.1$ fixed, the power increases with the plasma magnetization parameter σ_0 and first increases then decreases with the dominant X-point location r . Using the definition of η_c mentioned earlier, the critical value of the rotation parameter a_c is determined by solving the equation $\eta = -\frac{2}{27} \left(\sqrt{4M^2 - 3a_c^2} + 2M \right)^2 \left(\sqrt{4M^2 - 3a_c^2} - M \right)$. For $a > a_c$, the maximum power approaches a thousand, which is far greater than the tens shown in the Kerr case. This characteristic indicates that the spacetime modifications caused by the deformation parameter η have increased the maximum power and are likely to further affect the energy extraction efficiency. Significantly, in Fig.5(c), when a is slightly greater than the critical value a_c , there will be a sudden decrease in the power curve due to a sudden change in its energy at infinity per enthalpy ϵ_-^∞ , as shown in the last one of Fig.2(d). In Fig.6-7, with the plasma magnetization parameter $\sigma_0 = 100$ fixed, we plot the curves of power variation with the dominant X-point location r and the deformation parameter η . In Fig.6, for $\eta < 0$, the power increases with the rotation parameter a . For $\eta > 0$, the peak power significantly increases for large a and continues to rise as η increases. In Fig.7, the curve drawn from purple to red corresponds to $r = 1.1, 1.2, 1.3, 1.4, 1.5$. For the rotation parameter $a \leq M$, the power decreases with the deformation parameter η . However, for $a > M$, the power initially increases slowly

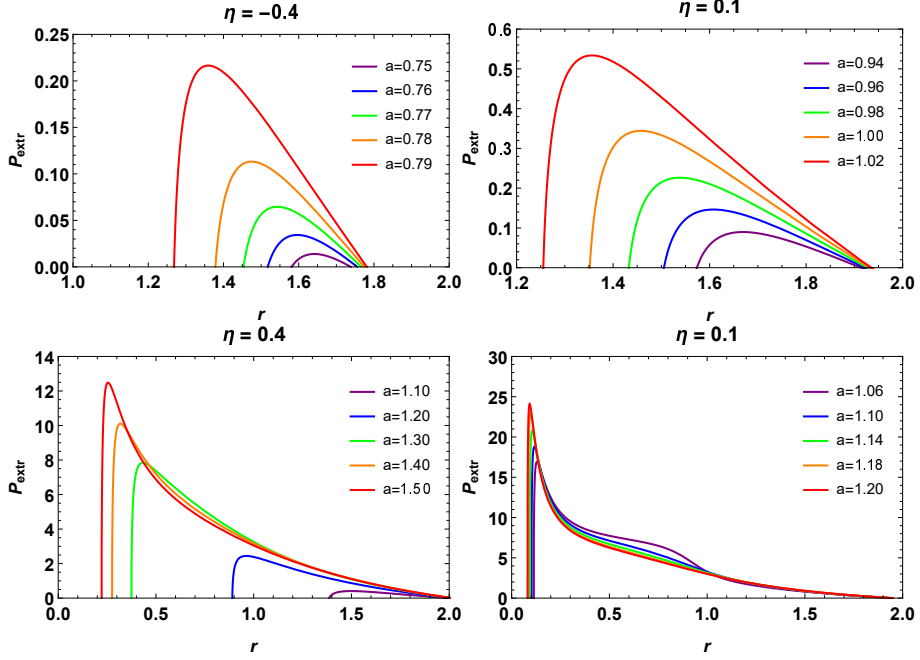


FIG. 6: The change of power P_{extr} with the dominant X-point location r for different rotation parameter a and deformation parameter η . We set $\sigma_0 = 100$ and $M = 1$.

and then sharply decreases to zero with the deformation parameter η increases. Notably, when the rotation parameter $M < a < \frac{2\sqrt{3}}{3}M$, the curve exhibits a sudden drop in the middle. This is due to the fact that as the deformation parameter increases, the photosphere radii rapidly grown from a very small value close to M , causing a sudden decrease in the cross-sectional area of the inflowing plasma A_{in} and leading to a sharp drop in the power of magnetic reconnection.

Through the process of magnetic reconnection, most of the magnetic energy is converted into the kinetic energy of the plasma. The plasma with the energy at infinity per enthalpy ϵ_+^∞ and ϵ_-^∞ escapes from the reconnection layer along the outflow directions of corotating and counter rotating motions. If the plasma particles with negative energy ϵ_-^∞ fall past the outer event horizon into the black hole along the corotating direction while the plasma particles with positive energy ϵ_+^∞ escapes to infinity along the counter rotating direction and carry away more energy, the efficiency of energy extraction via magnetic reconnection can be defined as [26]

$$\chi = \frac{\epsilon_+^\infty}{\epsilon_+^\infty + \epsilon_-^\infty}, \quad (29)$$

In Fig.8-9, we plot the variation of the efficiency of the energy extraction via magnetic reconnection with the dominant X-point location r and the deformation parameter η from a Konoplya-Zhidenko rotating non-Kerr

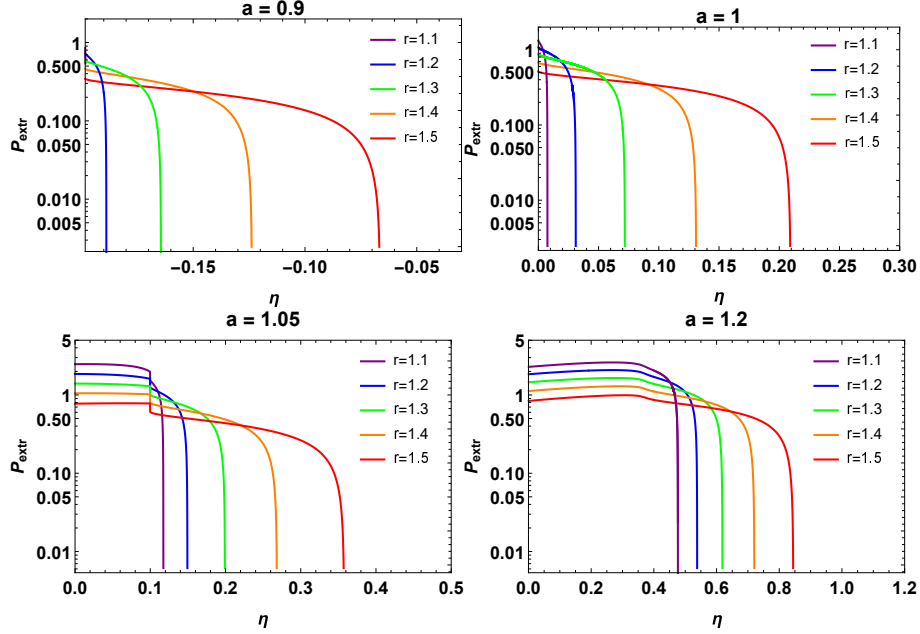


FIG. 7: The change of power P_{extr} with the deformation parameter η for different rotation parameter a and dominant X-point location r . We set $\sigma_0 = 100$ and $M = 1$.

black hole. From Fig.8(a)-(c), we observe that the efficiency of energy extraction initially increases and then decreases with the dominant X-point location r , resulting in a peak in the middle of the curve. When the deformation parameter $\eta \leq 0$, this peak increases with a . However, when $\eta > 0$, the rotation parameter a can extend beyond the region where $a > M$, and the peak initially rises then decreases with a . In Fig.8(d), when $0 < \eta \leq \frac{8}{27}$ and a is slightly greater than a_c , the curve exhibits a distinctive phenomenon of discontinuous intervals, with the endpoints of these intervals showing a sharp increase in efficiency towards infinity. This occurs because $\epsilon_+^\infty + \epsilon_-^\infty$ and the efficiency becomes negative within the discontinuous interval, while at the discontinuous endpoints, $\epsilon_+^\infty + \epsilon_-^\infty$ tends towards zero and the efficiency approaching an almost unlimited value. In Fig.9(a)-(c), the curve drawn from purple to red corresponds to $r = 1.1, 1.2, 1.3, 1.4, 1.5$. At the fixed dominant X-point location $r > M$, the efficiency decreases with the deformation parameter η in the cases of $a = 0.9$ and $a = 1.0$, but it first increases and then decreases with the deformation parameter in the cases of $a = 1.05$ and $a = 1.2$. In Fig.9(d), when the rotation parameter $M < a \leq \frac{2\sqrt{3}}{3}M$ and the dominant X-point location r is slightly greater than r_c , the efficiency increases first and then decreases with the deformation parameter, and its peak can reach so high that it is almost unlimited as shown in Fig.8(d). The energy extraction efficiency under magnetic reconnection in Kerr black hole can only approach $3/2$ [26], indicating that the existence of deformation parameter η in the Konoplya-Zhidenko rotating non-Kerr black hole greatly raises the upper limit of energy extraction efficiency under magnetic reconnection. The Penrose

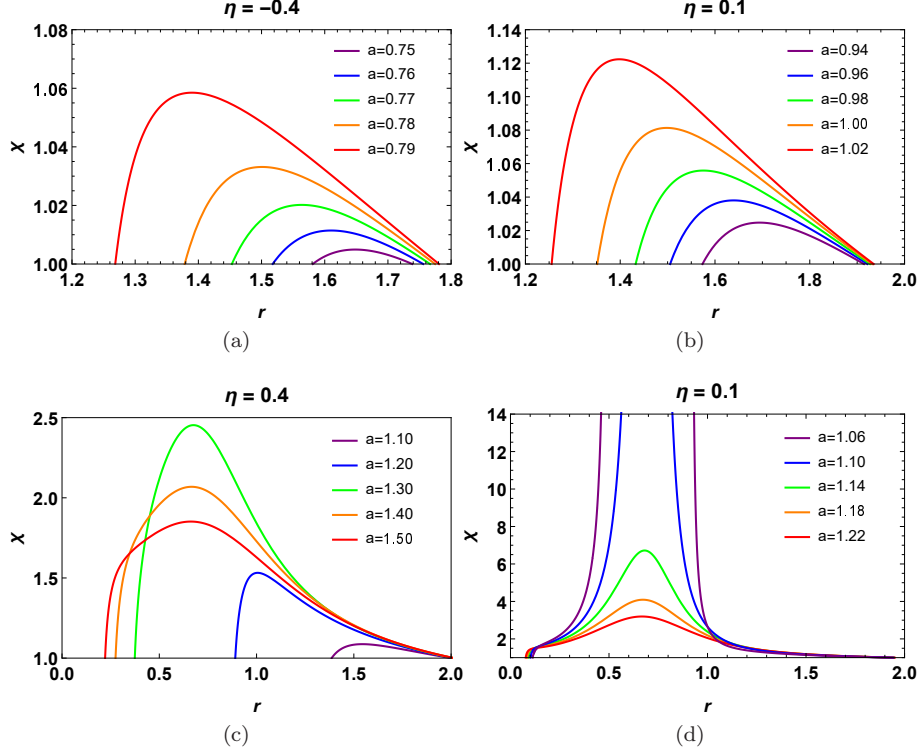


FIG. 8: The variation of the efficiency of the energy extraction via magnetic reconnection with the dominant X-point location r . We set $\sigma_0 = 100$ and $M = 1$.

process in the Konoplya-Zhidenko rotating non-Kerr black hole also yielded similar results, with the maximum efficiency approaching an almost unlimited value as the positive deformation parameter approaches zero and the incident particle splits near the horizon[44]. Since the maximum efficiency of energy extraction via magnetic reconnection requires the dominant X-point location to be close to r_c rather than the extremely small event horizon radius, achieving maximum efficiency through the magnetic reconnection process can be easier than the Penrose process.

Next, we will compare the power extracted from a Konoplya-Zhidenko rotating non-Kerr black hole via magnetic reconnection with the Blandford-Znajek process. The Blandford-Znajek process extracts rotational energy through a magnetic field threading the event horizon of a black hole, and the rate of energy extraction is expressed as:

$$P_{\text{BZ}} \simeq \kappa \Phi_{\text{BH}}^2 (\Omega_H^2 + \zeta_1 \Omega_H^4 + \zeta_2 \Omega_H^6), \quad (30)$$

where $\zeta_1 \approx 1.38$ and $\zeta_2 \approx -9.2$ are the numerical coefficients and $\kappa \approx 0.05$ is a numerical constant related to the magnetic field configuration. The angular velocity at the event horizon of Konoplya-Zhidenko black hole formulated as $\Omega_H = a/(r_+^2 + a^2)$. The magnetic flux passing through one hemisphere of the black hole horizon

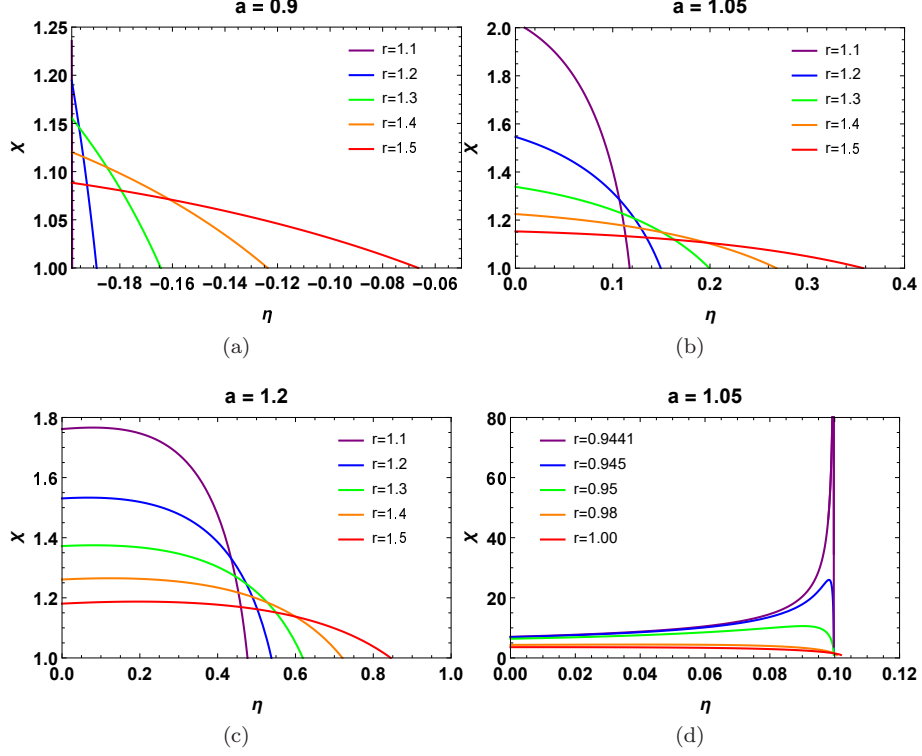


FIG. 9: The variation of the efficiency of the energy extraction via magnetic reconnection with the deformation parameter η . We set $\sigma_0 = 100$ and $M = 1$.

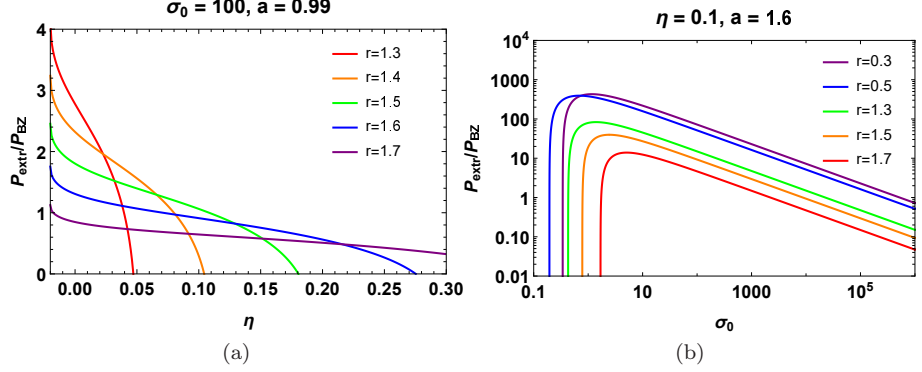


FIG. 10: The variation of the power ratio between magnetic reconnection and the Blandford-Znajek process with the deformation parameter η and the plasma magnetization parameter σ_0 . We set $M = 1$.

can be expressed as $\Phi_{BH} = \frac{1}{2} \int_{\theta} \int_{\phi} |B^r| dA_{\theta\phi} \sim \pi \int_0^{\pi} |B^r| \sqrt{-g} d\theta \sim 2\pi(r_+^2 + a^2)B_0 \sin \xi$. Therefore, the power ratio between magnetic reconnection and the Blandford-Znajek process can be written as [27]

$$\frac{P_{\text{extr}}}{P_{\text{BZ}}} \sim \frac{-4\epsilon_{-}^{\infty} A_{\text{in}} U_{\text{in}}}{\pi \kappa \sigma_0 (r_+^2 + a^2)^2 \sin^2 \xi (\Omega_H^2 + \zeta_1 \Omega_H^4 + \zeta_2 \Omega_H^6)}. \quad (31)$$

In Fig.10(a), the curve drawn from purple to red corresponds to $r = 1.3, 1.4, 1.5, 1.6, 1.7$ with $a = 0.99$. For

the rotation parameter $a \leq M$, the power ratio between magnetic reconnection and the Blandford-Znajek process decreases with the deformation parameter η , indicating that the presence of this parameter in the Konoplya-Zhidenko rotating non-Kerr black hole reduces the ratio compared to the Kerr case. In Fig.10(b), we plot the curve of the ratio as a function of the plasma magnetization parameter σ_0 . For the rotation parameter $a > M$, the dominant X-point location can be extended to small value, and the ratio increases significantly, becoming much greater than that in the Kerr black hole.

V. SUMMARY

In this paper we have investigated the energy extraction through the magnetic reconnection from a Konoplya-Zhidenko rotating non-Kerr black hole with an extra deformation parameter, analyzed the influence of deformation parameter on the possible region of the phase space, the power, the efficiency, and the power ratio of energy extraction in magnetic reconnection.

Firstly, to study energy extraction via the magnetic reconnection mechanism, it is essential to clarify the possible parameter regions where energy extraction can occur. For the case with $\eta \leq 0$, the rotation parameter of the black hole is limited to $a \leq M$, and the possible region of the phase space (a, r) for energy extraction shrinks as the deformation parameter increases. For the case with $\eta > 0$, the black hole can exhibit the superspinning case with $a > M$, allowing the phase space to extend into a wider area with $a > M$ and $r < M$, which are beyond the phase space (a, r) in a Kerr black hole. The energy extraction power and efficiency through magnetic reconnection in this expansion region are likely to exhibit fascinating characteristics.

Then we find that the power through the magnetic reconnection mechanism from a Konoplya-Zhidenko rotating non-Kerr black hole increases first and then decreases with the dominant X-point location r . For the case with $a \leq M$, the power decreases with the deformation parameter η . For the superspinning case with $a > M$, the power initially increases slowly and then sharply decreases with η . The maximum power in the Konoplya-Zhidenko rotating non-Kerr black hole approaches a thousand, which is greater than the Kerr case. Especially when the rotation parameter $M < a < \frac{2\sqrt{3}}{3}M$, there is a sudden drop in power due to the sharply increases in the radius of the photosphere as the deformation parameter increases.

The efficiency of the energy extraction via the magnetic reconnection initially increases and then decreases with the dominant X-point location r . At the fixed dominant X-point location $r > M$, the efficiency decreases with the deformation parameter η in cases with a higher rotation parameter a , but in superspinning cases, it first increases and then decreases with η . When the rotation parameter $M < a \leq \frac{2\sqrt{3}}{3}M$, the maximum

efficiency can become nearly unlimited, which is far greater than the maximum efficiency of $3/2$ in Kerr black hole. This indicates that the existence of deformation parameter in a Konoplya-Zhidenko rotating non-Kerr black hole significantly raises the upper limit of energy extraction efficiency. Since the maximum efficiency of energy extraction via magnetic reconnection requires the dominant X-point location close to r_c , while the Penrose process requires particle splitting to occur as close as possible to the extremely small event horizon, achieving maximum efficiency through the magnetic reconnection process can be easier than through the Penrose process in a Konoplya-Zhidenko rotating non-Kerr black hole.

Finally, we calculated the power ratio between magnetic reconnection and the Blandford-Znajek process. For the case with $a \leq M$, the power ratio decreases with the deformation parameter η , indicating that the presence of the deformation parameter reduces the ratio in the Konoplya-Zhidenko rotating non-Kerr black hole. For the superspinning case with $a > M$, the dominant X-point location can be extended to a smaller value and the ratio increases significantly, becoming much greater than the Kerr case.

In conclusion, the positive deformation parameters in the Konoplya-Zhidenko rotating non-Kerr black hole expand the possible region of energy extraction via magnetic reconnection to $a > M$ and $r < M$, improving the maximum power, maximum efficiency, and the maximum ratio between magnetic reconnection and the Blandford-Znajek process of energy extraction. Therefore, the Konoplya-Zhidenko rotating non-Kerr black hole can extract more energy via magnetic reconnection than Kerr black hole. These effects of the deformation parameter may provide valuable clues for future astronomical observations of black holes and verification of gravity theories.

VI. ACKNOWLEDGMENTS

This work was partially supported by the National Natural Science Foundation of China (Grant Nos. 12205140, 12275078, 11875026, 12035005, and 2020YFC2201400) and the Natural Science Foundation of Hunan Province (Grant No. 2023JJ40523).

-
- [1] B. P. Abbott, et al., Phys. Rev. Lett. **116**, 061102 (2016), arXiv:1602.03837.
 - [2] B. P. Abbott, et al., Phys. Rev. Lett. **116**, 241103 (2016), arXiv:1606.04855.
 - [3] B. P. Abbott, et al., Phys. Rev. Lett. **118**, 221101 (2017), arXiv:1706.01812.
 - [4] B. P. Abbott, R. Abbott, et al., Phys. Rev. Lett. **119**, 141101 (2017), arXiv:1709.09660.
 - [5] B. P. Abbott, et al., Astrophys. J. **851**, L35 (2017), arXiv:1711.05578.

- [6] K. Akiyama, et al. (The Event Horizon Telescope Collaboration), *Astrophys. J. Lett.* **875**, L1 (2019).
- [7] K. Akiyama, et al. (The Event Horizon Telescope Collaboration), *Astrophys. J. Lett.* **930**, L12 (2022).
- [8] J. C. McKinney and C. F. Gammie, *Astrophys. J.* **611**, 977 (2004).
- [9] J. F. Hawley and J. H. Krolik, *Astrophys. J.* **641**, 103 (2006).
- [10] S. S. Komissarov and J. C. McKinney, *Mon. Not. R. Astron. Soc.* **377**, L49 (2007).
- [11] A. Tchekhovskoy, R. Narayan and J. C. McKinney, *Mon. Not. R. Astron. Soc.* **418**, L79 (2011).
- [12] H. K. Lee, R. A. M. J. Wijers and G. E. Brown, *Phys. Rep.* **325**, 83 (2000).
- [13] A. Tchekhovskoy, J. C. McKinney and R. Narayan, *Mon. Not. R. Astron. Soc.* **388**, 551 (2008).
- [14] S. S. Komissarov and M. V. Barkov, *Mon. Not. R. Astron. Soc.* **397**, 1153 (2009).
- [15] A. R. King, M. B. Davies, M. J. Ward, G. Fabbiano, and M. Elvis, *Astrophys. J.* **552**, L109 (2001).
- [16] R. Penrose, *Riv. Nuovo Cimento Spec.* **1**, 252 (1969).
- [17] J. M. Bardeen, W. H. Press, S. A. Teukolsky, *Astrophys. J.* **178**, 347 (1972).
- [18] S. M. Wagh, S. V. Dhurandhar, N. Dadhich, *Astrophys. J.* **290**, 12 (1985).
- [19] S. Parthasarthy, S. M. Wagh, S. V. Dhurandhar and N. Dadhich, *Astrophys. J.* **307**, 38 (1986).
- [20] M. Bhat, S. Dhurandhar and N. Dadhich, *J. Astrophys. Astron.* **6**, 85 (1985).
- [21] R. D. Blandford and R. L. Znajek, *Mon. Not. R. Astron. Soc.* **179**, 433 (1977).
- [22] T. Piran, J. Shaham, and J. Katz, *Astrophys. J. Lett.* **196**, L107 (1975).
- [23] M. Takahashi, S. Nitta, Y. Tatematsu, and A. Tomimatsu, *Astrophys. J.* **363**, 206 (1990).
- [24] S. A. Teukolsky and W. H. Press, *Astrophys. J.* **193**, 443 (1974).
- [25] S. Koide and K. Arai, *Astrophys. J.* **682**, 1124 (2008).
- [26] L. Comisso and F. A. Asenjo, *Phys. Rev. D* **103**, 023014 (2021), arXiv:2012.00879.
- [27] S.-W. Wei, H.-M. Wang, Y.-P. Zhang, and Y.-X. Liu, *J. Cosmol. Astropart. Phys.* **04**, 050 (2022), arXiv:2201.12729.
- [28] M. Khodadi, *Phys. Rev. D* **105**, 023025 (2022), arXiv:2201.02765.
- [29] A. Carleo, G. Lambiase, and L. Mastrototaro, *Eur. Phys. J. C* **82**, 776(2022), arXiv:2206.12988.
- [30] W. Liu, *Astrophys. J.* **925**, 149 (2022), arXiv:2204.07338.
- [31] C. H. Wang, C. Q. Pang, and S. W. Wei, *Phys. Rev. D* **106**, (2022) 124050, arXiv:2209.08837].
- [32] Z. Li, X. K. Guo, and F. Yuan, *Phys. Rev. D* **108**, 044067 (2023), arXiv:2304.08831.
- [33] Z. Li and F. Yuan, *Phys. Rev. D* **108**, 024039 (2023), arXiv:2304.12553.
- [34] X. Ye, C. H. Wang, S. W. Wei, *J. Cosmol. Astropart. Phys.* **12** 030 (2023), arXiv:2306.12097.
- [35] M. Khodadi, D. F. Mota, and A. Sheykhi, *J. Cosmol. Astropart. Phys.* **10** 034 (2023), arXiv:2307.00478.
- [36] S. Shaymatov, M. Alloqulov, B. Ahmedov, and A. Wang, *Phys. Rev. D* **110**, 044005 (2024), arXiv:2307.03012.
- [37] S. J. Zhang, *Phys. Rev. D* **109**, 084066 (2024), arXiv:2402.15050.
- [38] S. J. Zhang, arXiv:2405.16941.
- [39] B. Chen, Y. Hou, J. Li, Y. Shen, arXiv:2405.11488.
- [40] Y. Shen, H. Y. YuChih, B. Chen, arXiv:2409.07345.
- [41] R. Konoplya and A. Zhidenko, *Phys. Lett. B* **756** 350 (2016).
- [42] C. Bambi and S. Nampalliwar, *Europhys. Lett.* **116**, 30006 (2016). arXiv:1604.02643.
- [43] Y. Ni, J. Jiang and C. Bambi, *J. Cosmol. Astropart. Phys.* **09**, 014 (2016).
- [44] F. Long, S. Chen, S. Wang and J. Jing, Energy extraction from a Konoplya-Zhidenko rotating non-Kerr black hole, *Nucl. Phys. B* **926**, 83 (2018), arXiv:1707.03175.